THE JOURNAL OF BIOLOGICAL CHEMISTRY VOL. 283, NO. 20, pp. 13825–13833, May 16, 2008

Inactivation of NuRD Component Mta2 Causes Abnormal T Cell Activation and Lupus-like Autoimmune Disease in Mice*

Received for publication, February 19, 2008, and in revised form, March 18, 2008 Published, JBC Papers in Press, March 19, 2008, DOI 10.1074/jbc.M801275200

Xiangdong Lu[‡§], Grigoriy I. Kovalev[¶], Hua Chang[‖], Eric Kallin[‡§], Geoffrey Knudsen[¶], Li Xia[‡§], Nilamadhab Mishra[**], Phillip Ruiz[‡‡], En Li[‖], Lishan Su[¶1], and Yi Zhang[‡§2]

*From the [‡]Howard Hughes Medical Institute, Departments of [§]Biochemistry and Biophysics and [¶]Microbiology and Immunology, University of North Carolina, Chapel Hill, North Carolina 27599, the [‖]Models of Disease Center, Novartis Institutes for Biomedical Research Inc., Cambridge, Massachusetts 02139, the **Department of Internal Medicine, Wake Forest University School of Medicine, Winston-Salem, North Carolina 27157, and the [‡‡]Department of Pathology, University of Miami, Miami, Florida 33136*

Dynamic changes in chromatin structure through ATP-dependent remodeling and covalent modifications on histones play important roles in transcription regulation. Among the many chromatin modifiers identified, the NuRD (nucleosome remodeling histone deacetylase) complex is unique because it possesses both nucleosome remodeling and histone deacetylase activities. To understand the biological function of the NuRD complex, we generated a knock-out mouse model of the *Mta2* (metastasis-associated protein 2) gene, which encodes a NuRD-specific component. *Mta2* null mice exhibited partial embryonic lethality. The surviving mice developed lupus-like autoimmune symptoms including skin lesions, bodyweight loss, glomerulonephritis, liver inflammation, and production of autoantibodies. Transplantation of bone marrow cells from *Mta2* null mice recapitulated some of the symptoms including skin lesion and bodyweight loss in the recipient mice. *Mta2* null T lymphocytes showed normal development but hyperproliferation upon stimulation, which correlates with hyperinduction of interleukin (IL)-2, IL-4, and interferon (IFN)-γ. T cell hyperproliferation, but not other autoimmune symptoms, was observed in T cell-specific *Mta2* knock-out mice. *Mta2* null T cells produced more IL-4 and IFN-γ under Th2 activation conditions, but normal levels of IL-4 and IFN-γ under Th1 activation conditions. Furthermore, we found that *IL-4* is a direct target gene of Mta2. Our study suggests that Mta2/NuRD is involved in modulating *IL-4* and *IFN-γ* expression in T cell immune responses, and gene expression in non-T cells plays an important role in controlling autoimmunity.

Dynamic changes in chromatin structure through ATP-dependent remodeling and covalent histone modifications play important roles in regulating gene expression. Studies in recent years have identified many ATP-dependent chromatin remodeling and histone modifying enzymes (1–3). Among them, the NuRD (nucleosome remodeling histone deacetylase) complex is of special interest because it possesses both nucleosome remodeling and histone deacetylase activities (4).

The major components of the mammalian NuRD complex include Mi-2β, Mta2 (metastasis-associated protein 2), HDAC1/2,[3] RbAp46/48, and Mbd3 (5, 6). HDAC1/2 and RbAp46/48 form a deacetylase core complex that exists in both NuRD and the Sin3A histone deacetylase complex (6–8). However, Mi-2β, Mbd3, and Mta2 appear to be unique for the NuRD complex (4, 9). Mi-2β is an ATP-dependent nucleosome remodeling enzyme (10). Studies in *Drosophila* and *Caenorhabditis elegans* indicate that Mi-2β is involved in *Hox* gene silencing and somatic cell differentiation (11, 12). In mammalian cells, Mi-2β has been shown to interact with a master lymphocyte transcription factor Ikaros (13). Mbd3 is a member of the Mbd (methyl-CpG-binding domain) containing protein family. It interacts with Mbd2, which in turn can recruit the NuRD complex to repress transcription of methylated DNA (8, 14). Recent studies have also shown that *Mbd3* is required for pluripotency of embryonic stem cells (15, 16).

In mammalian cells, Mta2 belongs to the Mta protein family, which also includes Mta1 and Mta3. *In vitro* studies demonstrated that MTA2 positively regulates HDAC activity (8). The *C. elegans* Mta2 homolog, egl-27 together with other NuRD component homologs have been shown to antagonize the Ras signaling pathway during vulval development (17). In addition to Mta2, Mta3 has also been shown to form a complex with other NuRD components and play important roles in invasive growth of breast cancer cells through repressing *Snail* gene transcription, and in B cell differentiation through the Bcl-6 transcription repressor (9, 18). *Mta1* gene overexpression has been associated with cancer metastasis (19, 20), although whether it functions together with other NuRD components is not clear. Compared with *Mta1* and *Mta3*, *Mta2* is more ubiquitously expressed. It is likely that different Mta family members form different NuRD-like complexes with distinct functions.

* This work was supported, in whole or in part, by National Institutes of Health Grants GM63067 (to Y. Z.) and AI48407 and HL72240 (to L. S.). The costs of publication of this article were defrayed in part by the payment of page charges. This article must therefore be hereby marked "*advertisement*" in accordance with 18 U.S.C. Section 1734 solely to indicate this fact.

[1] To whom correspondence may be addressed: 100 West Dr., UNC-Chapel Hill, CB7295, Chapel Hill, NC 27599-7295. Fax: 919-966-8212; E-mail: lsu@med.unc.edu.

[2] Investigator of the Howard Hughes Medical Institute. To whom correspondence may be addressed: 100 West Dr., UNC-Chapel Hill, CB7295, Chapel Hill, NC 27599-7295. Fax: 919-966-4330; E-mail: yi_zhang@med.unc.edu.

[3] The abbreviations used are: HDAC, histone deacetylase; KO, knockout; WT, wild type; TKO, T cell-specific knockout; BMT, bone marrow transplantation; SCID, severe combined immunodeficiency; ChIP, chromatin immunoprecipitation; SLE, systemic lupus erythematosus; IL, interleukin; IFN, interferon; TCR, T cell receptor; ELISA, enzyme-linked immunosorbent assay; LN, lymph node; mAb, monoclonal antibody; FACS, fluorescence-activated cell sorter; dsDNA, double stranded DNA; ES cell, embryonic stem cell.

Chromatin remodeling and histone modifications have been shown to play crucial roles in transcription regulation in the immune system (21). Previous studies have established that during T helper (Th) cell differentiation, expression of specific transcription factors, such as T-bet and GATA3, and cytokines, such as IFN-γ and IL-4, are regulated at the chromatin level (21–23). For example, histone hyperacetylation has been observed at the *IFN-γ* regulatory region in Th1 cells and at the *IL-4* regulatory region in Th2 cells (24, 25). DNA demethylation at *IL-4* promoters and the regulatory region have also been observed in Th2 differentiation (23, 26). Even though it is well established that histone modification and chromatin remodeling play important roles in lymphocyte differentiation and activation, little is known about the identity of the corresponding enzymes. Several recent reports have indicated a role of the NuRD complex in these processes. For example, deficiency in Mbd2, a NuRD-interacting methyl-CpG-binding protein, results in abnormal Th cell differentiation and abnormal *IL-4* expression (27). Another NuRD interacting protein, Ikaros, has been shown to set thresholds for T cell activation and TCR-mediated T cell differentiation (8). However, a direct link between NuRD and T cell function has yet to be established.

To understand the *in vivo* function of Mta2/NuRD, we have generated Mta2 knock-out mice. *Mta2* null mice exhibit multiple phenotypes including partial embryonic lethality, development defects, and more interestingly, a lupus-like autoimmune disease. This report focuses on characterizing the autoimmune phenotypes and T lymphocyte function in adult *Mta2* null mice. Our data revealed the important role of Mta2/NuRD in regulating *IL-4* and *IFN-γ* expression during Th2-prone immune response and in regulating gene expression in non-T cells to control autoimmunity.

EXPERIMENTAL PROCEDURES

Generation of Mice Carrying $Mta2^{2lox}$ and $Mta2^{1lox}$ Alleles and Manipulation of Mice—The *Mta2* targeting vector included PGK-Neo and MC1-tk expression cassettes for positive and negative selection, respectively. Two FRT sites were inserted to each side of the PGK-Neo minigene for future removal of the expression cassette by FLP recombinase. Two loxP sites were inserted in introns 3 and 11, respectively, to flank the region including the PGK-Neo cassette and the genomic sequence from exons 4 to 11. Linearized *Mta2* targeting vector was electroporated into J1 ES cells (129SvJ) and selected in the presence of G418 and FIAU (1-(2′-deoxy-2′-fluoro-β-D-arabinofuranosyl)-5′-iodouracil). Correctly targeted ES cell clones identified by PCR screens were expanded and injected into C57Bl/6 blastocysts to obtain chimeric mice, which were then bred to C57Bl/6 to produce C57Bl/6/129SvJ hybrid F1 progeny carrying the $Mta2^{2lox}$ allele. Mice heterozygous for the $Mta2^{2lox}$ allele were crossed with EIIa Cre transgenic mice to generate mice carrying the $Mta2^{1lox}$ allele in which Cre recombinase-mediated loxP recombination had occurred and removed the PGK-Neo cassette as well as the genomic sequence from exons 4 to 11. The primers (set *a* in Fig. 1*B*) for genotyping *Mta2* wild-type (WT) and $Mta2^{2lox}$ alleles are the 5′ sequence 5′-GCTGAAGCAGACAGCAAAC-3′ and 3′ sequence, 5′-CATGCCAGGTTTTGAACCC-3′. PCR was performed as follows: 94 °C at 3 min followed by 35 cycles of: 94 °C for 30 s, 55 °C for 30 s, 72 °C for 45 s, and then one cycle at 72 °C for 7 min. A 390-bp fragment is derived from the mutant allele and a 335-bp fragment is derived from the wild-type allele. The primers (set *b* in Fig. 1*B*) for genotyping the $Mta2^{1lox}$ allele are the 5′ sequence, 5′-GCTGACAGTAATGCTCGTGAGT-3′ and the 3′ sequence, 5′-ATGCTTCTCACTGAGCTACAGC-3′, and the fragment is 1.2-kb. PCR was performed as follows: 94 °C for 3 min followed by 35 cycles of: 94 °C for 30 s, 60 °C for 45 s, 72 °C for 90 s, and then one cycle at 72 °C for 7 min. A 1.5-kb fragment is derived from the $Mta2^{1lox}$ allele.

The *Mta2* null and control mice described in this report were on a mixed genetic background (129SvJ and C57Bl/6). *EIIa-Cre* (28) transgenic mice were purchased from the Jackson Laboratory and the *LckCre* transgenic mice were obtained from the laboratory of Zhuang Yuan at Duke University (24). The mouse maintenance and experiments were done following the University of North Carolina Institutional Animal Care and Use Committee approved protocols. The skin and liver tissues from control and Mta2 knock-out mice were fixed in formalin for 20–24 h and embedded in paraffin. Tissue sections (5 μm) were stained with hematoxylin and eosin (H&E) for morphological examination.

ELISA—Serum was collected from *Mta2* null and control mice of different ages. Serum anti-dsDNA, anti-Sm, anti-SSA, and anti-SSB antibodies levels were measured using ELISA kits from Alpha Diagnostics International Inc. (San Antonio, TX).

Flow Cytometry Analysis of Lymphoid Population—Age-matched conventional *Mta2* null, T cell-specific null, and age- and sex-matched control mice were used for analysis. Single cell suspensions of thymocytes, spleen cells, and lymph node (LN) cells were stained with fluorescein isothiocyanate (FITC)-, phycoerythrin (PE)-, peridinin chlorophyll protein (PerCP)-, and allophycocyanin (APC)-conjugated monoclonal antibodies and analyzed with FACSCalibur (BD Biosciences). All the antibodies used for immunostaining were purchased from BD Biosciences. Data were analyzed using SUMMIT software.

T Cell Proliferation, Th Polarization, and Cytokine Assay—T cell proliferation assay was performed using a previously described protocol (29). Briefly, cervical, umbilical, and axial lymph nodes from each mouse were harvested and pooled. About 5×10^5 LN cells or 1×10^5 purified $CD4^+CD25^-$ T cells were plated in each well of a 96-well plate. The plate was previously coated with goat anti-hamster antibody (10 μg/ml). Thirty-six to 48 h later, the cells were pulsed with [^{3}H]thymidine and harvested after 12 h of incubation. For cytokine production assay, about 2×10^6 anti-CD3/anti-CD28 mAb-stimulated LN cells were plated in a 24-well plate and cultured for 4 days before harvesting of the supernatant. The cytometric bead array was performed according to manufacturer's instruction (BD Biosciences). For Th differentiation, $CD4^+$ T cells were purified from pooled spleen and LN cells using the $CD4^+$ purification kit follow up AutoMACS^{TM} cell separation (Miltenyi Biotec Inc., Auburn, CA). 2×10^6 $CD4^+$ cells were stimulated with anti-CD3 and anti-CD28 mAb, as described, in the presence of recombinant human IL-2 (100units/ml) (nonpolarized condition). In addition, for Th1 differentiation, cells were stimulated in the presence of recombinant mouse IL-12 (5 ng/ml)

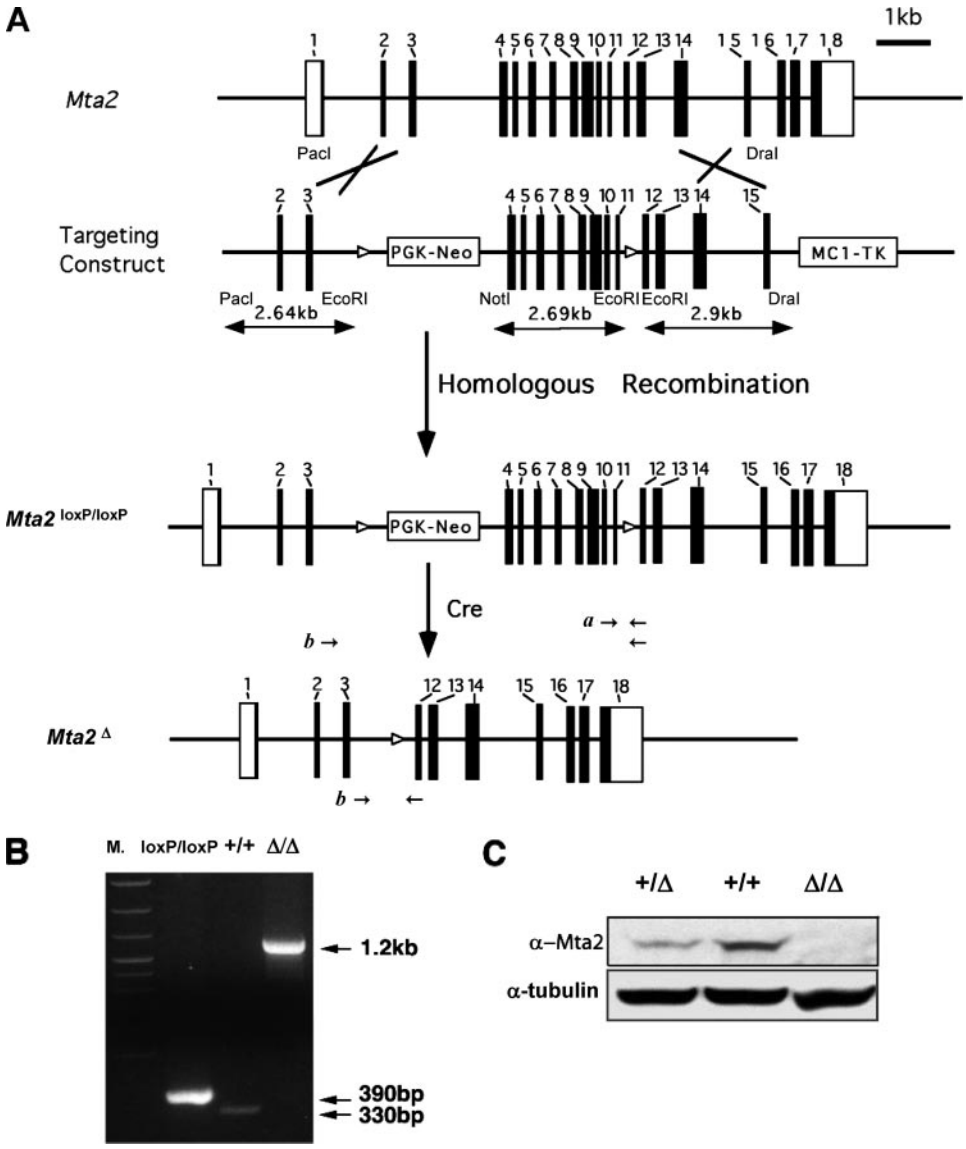

FIGURE 1. **Generation of *Mta2* mutant mice.** *A*, schematic representation of the *Mta2* wild-type locus, the targeting vector, the *Mta2*^{2lox} allele, and the *Mta2*^{1lox} allele. The targeting vector contains two loxP sites (*open triangle*) that flank exons 4 to 11, and two expression cassettes, PGK-Neo and MC1-TK for positive and negative selection in ES cells. After the targeting construct is electroporated into ES cells, homologous recombination events were analyzed by PCR with two primer sets indicated as *a* and *b*. A third set of primers, *c*, is used to screen the *Mta2*^{1lox} allele, which is generated after Cre-mediated loxP recombination occurs in the *Mta2*^{2lox} allele. Cre-mediated excision of exons 4–11 generates a frameshift in exon 12. As a result, the mutant transcript only encodes the 63 N-terminal amino acids of Mta2. *B*, the three alleles of *Mta2*, namely, the wild-type allele (+/+), the *Mta2*^{2lox} allele, and the *Mta2*^{1lox} allele are distinguished by PCR. *C*, Western blot analysis with anti-Mta2 antibody using liver protein extracts from wild-type (+/+), heterozygous (+/Δ), and *Mta2* knock-out mice (Δ/Δ). Mta2 protein was not detectable in *Mta2* null mice. Tubulin was used as a loading control.

TABLE 1
Inactivation of the *Mta2* gene causes partial embryonic lethality

Numbers and percentages of newborn mice with three possible *Mta2* genotypes (+/+, +/−, and −/−) from *Mta2*$^{+/-}$ breeding pairs or male *Mta2*$^{-/-}$ and female *Mta2*$^{+/-}$ breeding pairs. The percentages of newborn *Mta2*$^{-/-}$ mice are significantly lower than Mendelian distribution ($p < 0.01$), indicating some *Mta2*$^{-/-}$ mice died at embryonic stage.

	Mta2 genotype		
	+/+	+/−	−/−
***Mta2*$^{+/-}$ × *Mta2*$^{+/-}$**			
Number	53	171	26
Percentage	21.2%	68.4%	10.4%
***Mta2*$^{-/-}$ × *Mta2*$^{+/-}$**			
Number		90	26
Percentage		77.6%	22.4%

and anti-IL-4 (4 μg/ml) (Pharmingen). For Th2 differentiation, cells were stimulated in the presence of mouse IL-4 (50 ng/ml), anti-IL-12 (5 μg/ml), and anti-IFN-γ (4 μg/ml) mAbs (Pharmingen). After 7 days of culture, cells were washed and stimulated with phorbol 12-myristate 13-acetate (10 ng/ml) and ionomycin (1 μM) for 6 h in the presence of BD GolgiPlug containing brefeldin A (Pharmingen) for the last 4 h. IL-4 and IFN-γ expression was assessed by intracellular staining. Harvested cells were stained with anti-CD4 mAb, permeabilized with BD FACS Permeabilizing Solution 2 (BD Bioscience), and stained with anti-IL4 and anti-IFN-γ mAbs. Samples were fixed with 1% paraformaldehyde and analyzed by FACSscan (BD Bioscience). 1×10^5 cells from each polarization condition were harvested and analyzed for *IL-4* expression by real-time PCR.

Reconstituted SCID Mice—To reconstitute SCID mice, bone marrow (BM) cells from 11-week-old *Mta2* WT and *Mta2* null mice were injected into irradiated (250R) SCID-NOD mice (5×10^6 bone marrow cells per mouse). LN T cells in the reconstituted mice were harvested at 8 weeks post-reconstitution, and standard FACS and T cell proliferation assays were performed.

Quantitative Real-time PCR—Total RNA was extracted using the Qiagen RNeasy mini kit as per the manufacturer's instructions. RNAs were denatured for 3 min at 70 °C and cDNAs were synthesized in Ambion RT buffer with random decamers and 100 units of Moloney murine leukemia virus reverse transcriptase (Invitrogen) for 1 h at 42 °C followed by 10 min at 95 °C to inactivate the enzyme. Real-time PCR analysis was performed using TaqMan primer/probe mixtures (Applied Biosystems) as recommended by the manufacturer and analyzed on an Applied Biosystems 7900HT system.

Chromatin Immunoprecipitation (ChIP) Assay—The ChIP assay was modified from a previously described protocol (24). The peripheral T cells were purified by the CD4$^+$ T cell purification kit (Miltenyi Biotec Inc., Auburn, CA). *IL-4* PCR primers were: 1 forward GCCAATCAGCACCTCTCTTC, 1 reverse, TAAAGCCTCATTCCATGGTC; 2 forward, CATCGCTACACCTCCCAC, 2 reverse, CCTTGGTTTCAGCAACTTTAAC.

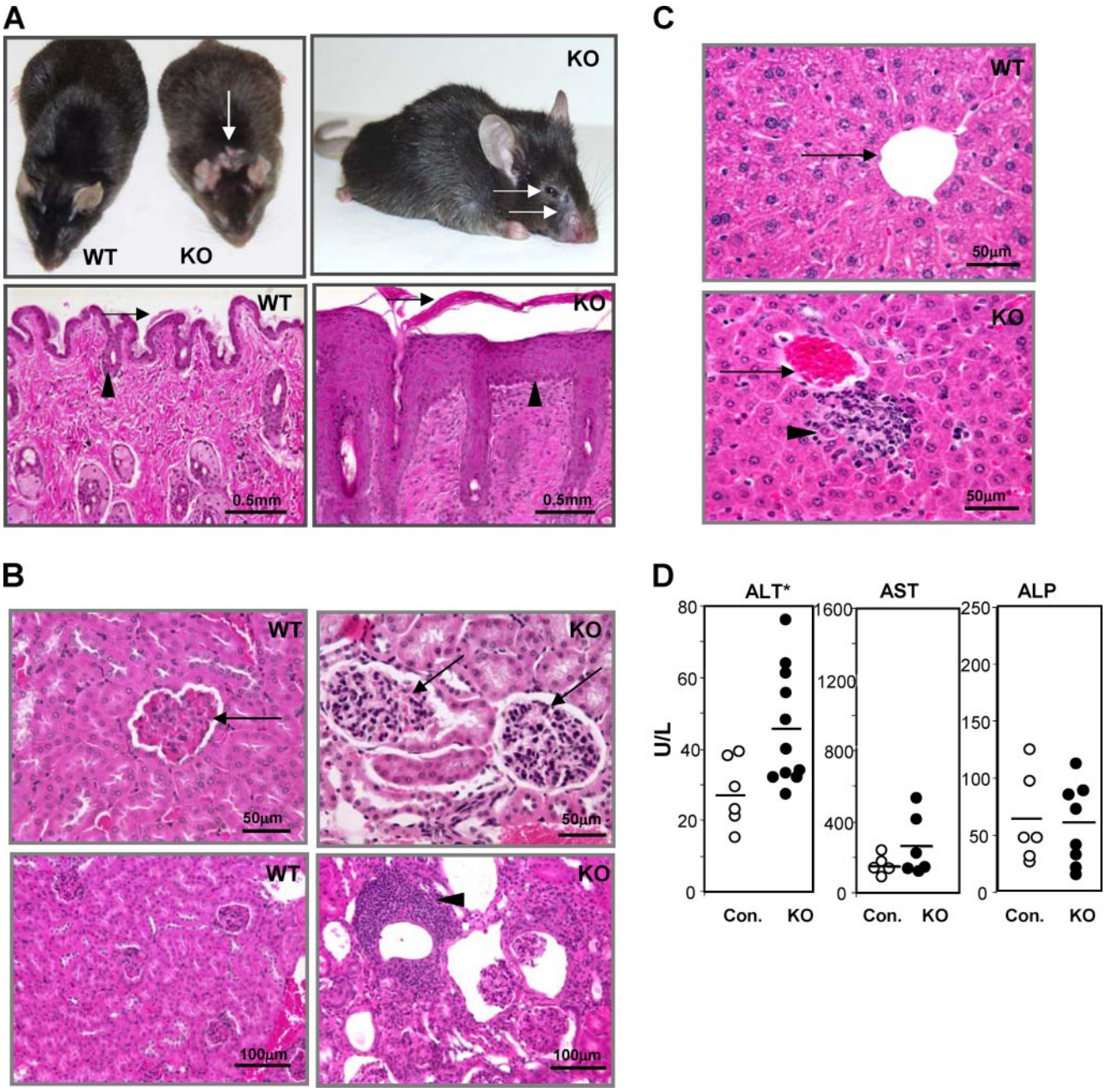

FIGURE 2. **Adult Mta2 knock-out (*KO*) mice exhibit autoimmunity-related phenotypes in multiple organs.** *A*, *upper panels*, *Mta2* KO mice show skin lesions at eyelid, mouth, nose, and neck area as indicated by *arrows*; *lower panels*, hemotoxylene and eosin (H&E) staining of skin sections from wild-type and *Mta2* null mice show significant hyperkerotosis (*arrow*) and epidermal cell hyperplasia (acanthosis) (*arrowheads*) in *Mta2* null mice. *B*, *upper panels*, H&E-stained kidney sections of *Mta2* null mice reveal mesangial cell proliferation (*arrowhead*); *lower panels*, *Mta2* null mice also show lymphocyte infiltration (*arrow*) in kidney. *C*, *Mta2* null mice develop liver inflammation. H&E-stained liver sections of *Mta2* null mice reveal lymphocyte infiltration (*lower panel*, *arrowhead*). Portal veins are indicated by *arrows*. *D*, comparison of the liver enzyme activity levels in serum measured by ELISA. *Mta2* null mice had a significantly increased alanine aminotransferase (*ALT*) level ($p < 0.01$), indicating liver cell damage in these mice. The mutant mice showed no significant change in the levels of aspartate aminotransferase (*AST*) and alkaline phosphatase (*ALP*) in the serum of *Mta2* null mice when compared with the wild-type mice. *Asterisk* indicates the difference is statistically significant.

Statistics—Chi-square tests were used for genotype distribution analysis. T tests were used for statistical analysis of mouse bodyweight, different type of T cell analysis, and T cell proliferation assay. Wilcoxon rank test was used for survival analysis.

RESULTS

Generation of the Mta2 Mutant Mice—Although the composition and biochemical properties of the mammalian NuRD complex have been extensively characterized (4), its biological function is not well understood. To gain insight into its function, we generated a mouse model in which a component of the NuRD complex is deleted by gene targeting. We chose to inactivate *Mta2* because the protein encoded by this gene appears to be present only in the NuRD complex. We made a conditional gene targeting vector in which *Mta2* exons 4–11 were flanked by two loxP sites (Fig. 1*A*). Cre-mediated recombination at these two loxP sites resulted in deletion of exons 4–11 and a frameshift in exon 12. As a result, the Mta2 mutant allele

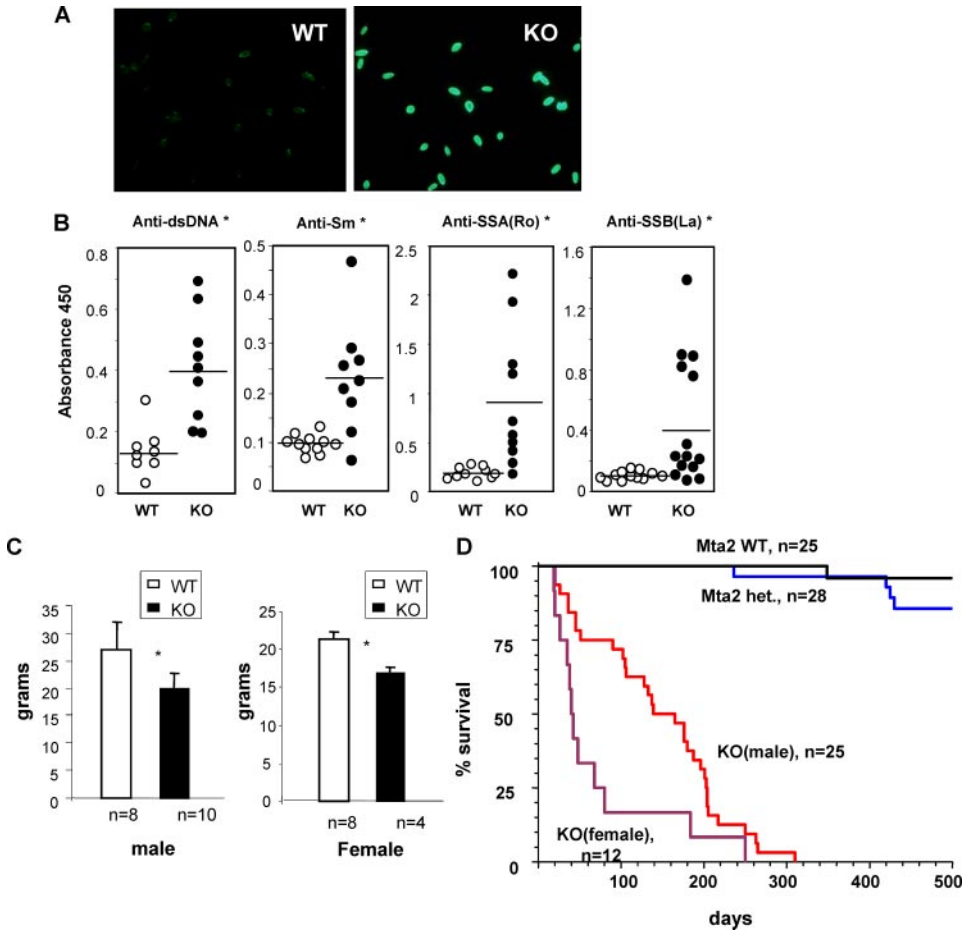

FIGURE 3. ***Mta2* null mice develop lupus specific autoantibodies.** *A*, production of anti-dsDNA antibody is detected by the *Crithidia Luciliae* assay that showed positive anti-dsDNA antibody in the *Mta2* null serum but not wild-type serum. *B*, ELISA analysis demonstrates significantly elevated levels of different autoantibodies, including anti-dsDNA, anti-Sm, anti-SSA, and anti-SSB, in *Mta2* null mice when compared with those of wild-type mice ($p < 0.02$). *C*, bodyweight of 2-month-old wild type and *Mta2* null mice are plotted according to their genders. The average bodyweight of null mice is about 75% of that of their wild-type litter mates. *D*, Kaplan-Meier survival analysis of *Mta2* null and control mice. *Mta2* null mice have much shorter lifespans when compared with wild-type or heterozygous mice. Female null mice have a shorter lifespan than the male null mice that is similar to what have been observed in lupus patients and murine lupus models. *Asterisk* indicates the difference is statistically significant ($p < 0.05$).

would only encode the N-terminal 63 amino acids of the Mta2 protein (Fig. 1*A*). To investigate the function of Mta2 in whole animal, the $Mta2^{2lox/+}$ mice were crossed with EIIa-Cre transgenic mice. The $Mta2^{1lox}$ mice carrying one completely recombined allele (equal to conventional heterozygous knock-out mice) were selected for breeding. The $Mta2^{1lox}$ mice will be referred to as *Mta2* heterozygous mice and the $Mta2^{1lox/1lox}$ mice will be referred to as *Mta2* null or *Mta2* conventional null mice in this report. As shown in Fig. 1*B*, the $Mta2^{2lox}$, $Mta2^{1lox}$, and *Mta2* wild-type allele can be distinguished by PCR. Western blot analysis of protein extracts derived from *Mta2* knock-out mice confirmed the lack of Mta2 protein (Fig. 1*C*).

Mta2 Knock-out Mice Exhibit Multiple Phenotypes Including Lupus-like Autoimmune Diseases—Inactivation of the *Mta2* gene caused embryonic and perinatal lethality in about half of *Mta2* null mice. Fewer than 50% of *Mta2* null mice (in 129/C57/B6 mixed genetic background) survived to adulthood (Table 1). Backcross of the *Mta2* null mice onto a C57/B6 background caused more severe embryonic lethality. The *Mta2* knock-out embryos exhibited defects in axial skeleton, skin, and craniofacial structure with different penetrance (data not shown). The *Mta2* null mice that survived postnatally exhibited smaller body size and female infertility.

Adult *Mta2* mice also developed erosive skin lesions at multiple locations with high penetrance. More than 90% of the *Mta2* null mice showed periorbital erosion by 1 month of age (Fig. 2, *A* and *B*). From 4 months of age, ~75% of *Mta2* null mice developed additional skin lesions in areas surrounding the mouth and nose, and about 30% of *Mta2* null mice showed skin lesions in the neck region (Fig. 2*A*, *upper panels*). Histological sections of skin from the neck lesions of the *Mta2* mutant mice revealed hyperkeratosis and acanthosis of epidermal cells, as well as a chronic inflammatory response (Fig. 2*A*, compare *two lower panels*). The periorbital skin from null mice also showed hyperkeratosis and inflammation. In some regions there were immature hair follicles and a reduced number of hair follicles although frank alopecia was not evident at these early stages. Often there was evidence of dermal and subcutaneous inflammation (panniculitis) and the overall changes could be characterized as a chronic spongiotic dermatitis. The similarity between the skin lesions of *Mta2* null mice and those of mice with lupus-like autoimmune disease (30, 31) implies possible defects in the immune system of the *Mta2* null mice.

A histological examination of internal organs revealed that most *Mta2* null mice developed global mesangial cell proliferation in kidney (Fig. 2*B*, compare *upper panels*) and some of them also showed a significant lymphocyte-rich chronic inflammatory cell infiltration (Fig. 2*B*, compare *lower panels*). These renal abnormalities are consistent with histopathological changes occurring with glomerulonephritis seen in murine lupus models. Consistent with above symptoms observed in *Mta2* null kidneys, about 40% of adult *Mta2* knock-out mice showed moderate (>30 mg/dL) or high (>100 mg/dL) urine protein levels ($n = 20$). Control mice showed only trace or negative urine protein levels. This phenotype is more severe in female null mice than in the male null mice. In addition, liver inflammation was also found in more than half of the adult *Mta2* null mice. The lymphocyte infiltration was generally limited to the portal regions (Fig. 2*C*).

Consistent with injury to hepatocytes in the *Mta2* null mice, ELISA results showed that the serum alanine aminotransferase

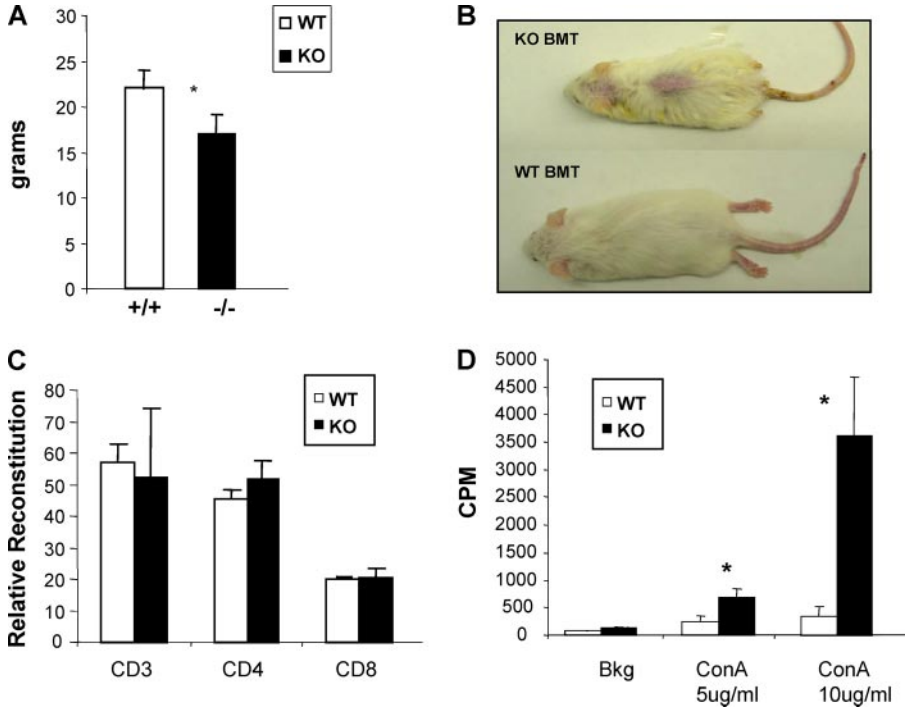

FIGURE 4. **Mta2-deficient BM cells cause decreased bodyweight, skin lesion, and T cell hyperproliferation in recipient SCID mice.** *A*, the transfer of BM cells from Mta2 knock-out (*KO*) mice cause 25% decreased bodyweight in recipient SCID mice 8 weeks after bone marrow transplantation ($p < 0.03$). *B*, a representative SCID mouse received *Mta2* KO BMT showed skin lesion (*upper mouse*), whereas the representative SCID mouse received BMT from wild-type mice exhibited normal skin (lower mouse) 8 weeks after transplantation. In this experiment, all three SCID mice that received Mta2 KO BM cells developed skin lesion and none of the four SCID mice received wild-type BM cells developed skin lesion. *C*, FACS analysis indicated that transplanted *Mta2* KO BM cells successfully reconstituted in T cells in SCID mice. The relative reconstitution of T cells from *Mta2* KO BMT SCID mice and WT BMT SCID mice were plotted ($n = 3$ for each genotype). *D*, the LN cells from *Mta2* KO BMT SCID mice showed hyperproliferation upon different concentrations of concanavalin A (*ConA*) stimulation. *Asterisk* indicates the difference is statistically significant ($p < 0.05$).

activity level is increased when compared with that of wild-type and heterozygous littermates (Fig. 2*D*). However, the activity levels of serum aspartate aminotransferase and alkaline phosphatase did not exhibit a significant difference between wild-type and *Mta2* null mice (Fig. 2*D*).

To further characterize the autoimmune disease observed in *Mta2* null mice, we collected serums from mutant and control mice at different ages and examined them for the different autoantibodies. The *Crithidia Luciliae* assay demonstrated the presence of anti-dsDNA antibody in the *Mta2* null serum (Fig. 3*A*). ELISA analysis showed significantly higher levels of anti-dsDNA, anti-Sm, anti-SSA, and anti-SSB antibodies (Fig. 3*B*). No difference in autoantibody level had been observed between *Mta2* heterozygous mice and wild-type mice. Anti-dsDNA and anti-Sm antibodies are markers of human and murine systemic lupus erythematosus (SLE), and anti-SSA and anti-SSB antibodies are often evident with Sjogren disease or SLE.

Furthermore, *Mta2* null mice are smaller than their littermates. The extent of difference depends on mouse development stages. From perinatal to weaning stage, *Mta2* null mice are about half to 2/3 size of the heterozygous or wild-type littermates. When they reach mature age (after 2 months old), both male and female null mice are about 75% of the size of their wild-type littermates (Fig. 3*C*). *Mta2* null mice also have shortened lifespans when compared with their wild-type or heterozygous littermates (Fig. 3*D*). Interestingly, female knock-out mice exhibit a shorter lifespan than male knock-out mice. Given that 90% of SLE patients are female (32), and some lupus mouse models have shown more severe phenotype in females than in males (33, 34), it is very likely that autoimmune-related symptoms are important factors causing early death in *Mta2* null mice. However, our results do not exclude other factors in causing premature death. In summary, our observations strongly suggest that *Mta2* null mice develop an autoimmune disease that resembles systemic lupus erythematosus in human.

Bone Marrow Transplantation Recipient Mice Partially Recapitulate the Autoimmune Phenotypes—To test if the autoimmune phenotypes observed in the *Mta2* null mice is caused by bone marrow derived from *Mta2* null cells; we transferred *Mta2* null bone marrow progenitor cells into SCID mice and monitored hematopoietic reconstitution over time. No significant defects were observed in lymphoid and myeloid reconstitution with *Mta2* mutant progenitor cells (data not shown). However, recipient mice transplanted with *Mta2* null hematopoietic stem and progenitor cell developed skin lesions and reduced body weight (Fig. 4, *A* and *B*), similar to *Mta2* null mice. When mice were analyzed 8–12 weeks post bone marrow transplantation, normal T cells were present in the thymus and peripheral lymphoid organs (Fig. 4*C*). However, these *Mta2* null T cells were hyperproliferative when stimulated with T cell mitogens (Fig. 4*D*). The phenotypes are, however, less severe compared with *Mta2* null mice, and no obvious liver inflammation or glomerulonephritis was detected in the transplanted mice. No increased level of autoantibodies was observed either (data not shown). These results indicate that hematopoietic cells derived from *Mta2* null bone marrow stem cells contribute to but are not sufficient to cause the autoimmune diseases. Therefore, non-hematopoietic cells must have also contributed to the autoimmune phenotypes of *Mta2* null mice.

T Cell Hyperproliferation in Mta2 Null Mice—The autoimmune phenotypes described above and previous reports on epigenetic regulation in T cell development and differentiation by some NuRD components prompted us to investigate possible T cell defects in *Mta2* null mice. We found that *Mta2* null mice exhibited normal T cell developments in thymus and peripheral lymphoid organs (Fig. 5*A*). The development of $FoxP3^+CD4^+CD25^+$ Treg cells and their functions are also not affected by loss of Mta2 (data not shown). Our data also indicated that the ratio of naïve T cells and memory T cells in

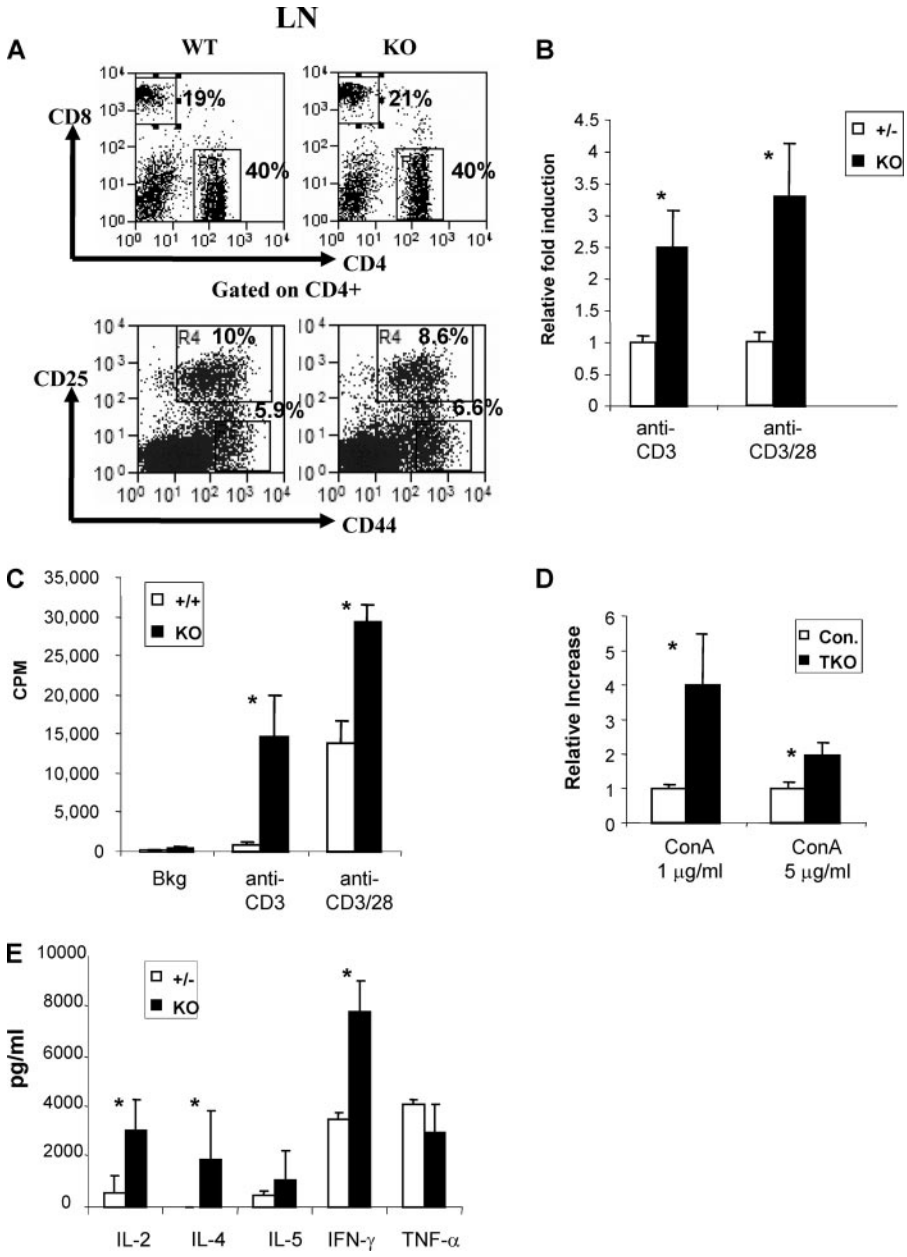

FIGURE 5. **Inactivation of *Mta2* gene causes intrinsic T cell hyperproliferation.** *A*, *Mta*2 null mice showed normal peripheral T cell development. Representative plots of FACS analysis for CD4/CD8 expression on LN cells (*upper*) and CD44/CD25 (*lower*) expression on $CD4^+$ LN cells. *B*, *Mta2* null LN cells are hyperproliferative in response to anti-CD3, or anti-CD3 and anti-CD28 mAb stimulation ($p < 0.01$). Heterozygous littermates were used as controls because no significant difference between heterozygous and wild-type mice has been observed. Data were collected from 5 independent experiments ($n = 7$ for each genotype). The average value obtained from heterozygous LN cells in each experiment is normalized to 1. *C*, peripheral $CD4^+CD25^-$ T cells were purified from *Mta2* null and wild-type mice, and then incubated and stimulated with anti-CD3 or anti-CD3 and anti-CD28 mAb antibodies. *Mta2* null $CD4^+CD25^-$ T cells were hyperproliferative compared with wild-type $CD4^+CD25^-$ T cells. *D*, T cells from T cell-specific knock-out (*KO*) mice are hyperproliferative. LN cells from *LckCre,Mta2*$^{2lox/lox}$ mice and *LckCre,Mta2*$^{2lox/2lox}$ mice and TKO are hyperproliferative when compared with LN cells from control mice (*Con.*) under concanavalin A (*ConA*) stimulation ($n = 4$ for each genotype, $p < 0.05$). Control mice include *LckCre, Mta2*$^{2lox/+}$, and *Mta2*$^{2lox/+}$ mice. *E*, cytokine analysis showed increased secretion of IL-2, IL-4, and IFN-γ by the *Mta2* null T cells upon anti-CD3/anti-CD28 mAb stimulation, but no significant difference has been observed in terms of the level of IL-5 or TNF-α ($n = 2$ for each genotype). *Asterisk* indicates the difference is statistically significant ($p < 0.05$).

Mta2-deficient peripheral lymphoid organs was normal (Fig. 5*A*). However, when stimulated with anti-CD3, or anti-CD3 in combination with anti-CD28 mAbs, *Mta2*-deficient T cells from LN were hyperproliferative compared with the LN T cells from control mice (Fig. 5*B*) ($n = 7$ for each genotype). Furthermore, purified $CD4^+CD25^-$ peripheral T cells from *Mta2* null mice also showed hyperproliferation in response to TCR stimulation (Fig. 5*C*). To evaluate whether the observed hyperproliferation is T cell autonomous, we have generated *LckCre, Mta2*$^{2lox/1lox}$, and *LckCre, Mta2*$^{2lox/2lox}$ mice that exhibit *Mta2* gene deletion in T cells. Similar to that observed in the conventional Mta2 null mice, T cells from T cell-specific *Mta2* null (TKO) mice also exhibited hyperproliferation upon T cell activation (Fig. 5*D*). However, no other autoimmune phenotypes were observed in these mice (data not shown), suggesting that non-T cells must have contributed to the autoimmune disease in the *Mta2* conventional null mice.

To understand the molecular basis of T cell hyperproliferation in response to *Mta2* inactivation, we analyzed the effects of *Mta2* inactivation on the levels of various cytokines induced by the LN-derived lymphocytes. Results shown in Fig. 5*E* indicate that *Mta2* null T cells produced more IL-2, IL-4, and IFN-γ than control cells when stimulated with anti-CD3 and anti-CD28 mAbs, consistent with hyperproliferation of *Mta2* null T cells.

Mta2 Regulates IL-4 and IFN-γ Production under Th2 Conditions—In response to Mta2 inactivation, both IFN-γ and IL-4 were hyperinduced in TCR-activated T cells (Fig. 5*E*). Given that epigenetic mechanisms are involved in silencing IL-4 and IFN-γ during T cell activation under Th1 or Th2 conditions, respectively (21–23), we asked whether Mta2 is involved in silencing of the *IL-4* and *IFN-γ* genes under Th1 or Th2 conditions. Results shown in Fig. 6*A* indicate *Mta2* inactivation did not affect Th1 polarization, suggesting that Mta2 is not involved in modulating IL-4 or IFN-γ expression during Th1 responses. However, expression of both IL-4 and IFN-γ in *Mta2* null T cells was elevated under Th2 conditions when compared with that of wild-type T cells (Fig. 6*B*). These results suggest

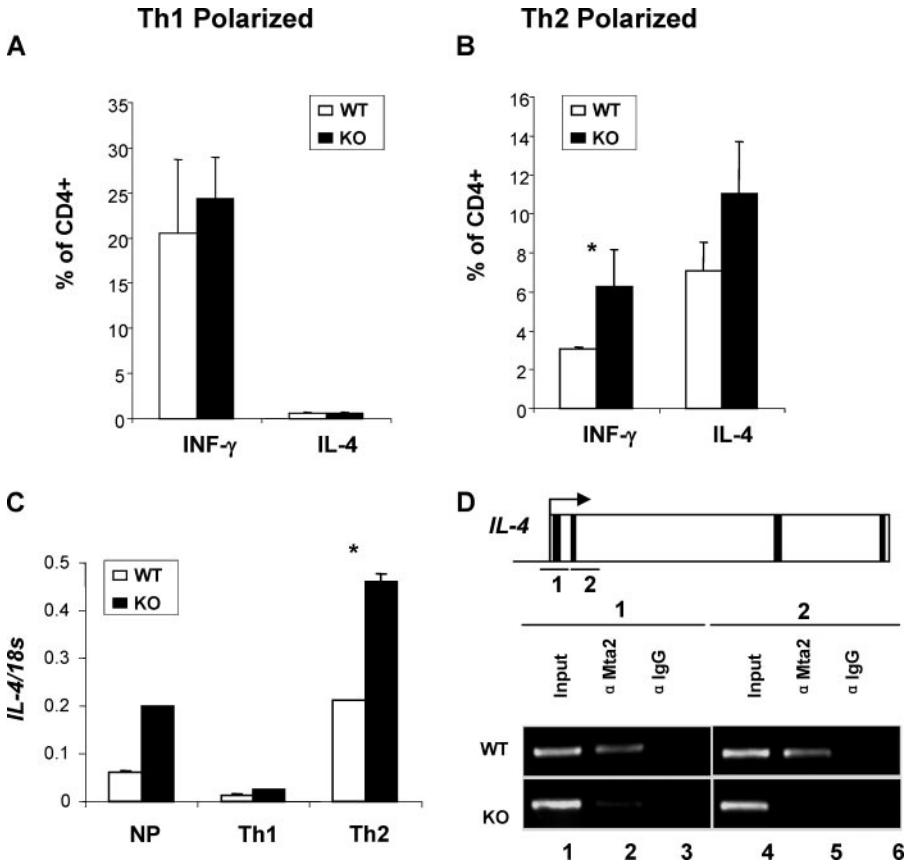

FIGURE 6. **IL-4 is a direct target of Mta2.** *A*, normal Th1 polarization in Mta2 null cells. *B*, loss of Mta2 function results in increased IFN-γ and IL-4 under Th2 conditions. Results of FACS analysis are shown on *A* and *B* as *bar graphs* representing percentage of IFN-γ^+ and IL-4^+ gated on $CD4^+$ cells. Data presented are an average of 3 mice per genotype from two independent experiments. Standard deviation is shown as *error bars*. *C*, real-time reverse transcriptase-PCR results of *IL-4* expression levels in cells activated under non-polarizing, Th1 or Th2 conditions. Results are expressed as the ratio of *IL-4* over 18 S to control for amounts of cDNA analyzed ($p < 0.01$). *D*, ChIP assays demonstrate that Mta2 is localized to the *IL-4* gene in the wild-type, but not in the *Mta2* null mice. Exons are indicated by *black strips*. *Asterisk* indicates the difference is statistically significant ($p < 0.05$).

that Mta2 is involved in suppressing expression of both IL-4 and IFN-γ during Th2 responses.

IL-4 Is a Direct Target of Mta2—Considering the fact that Mta2/NuRD is a co-repressor complex (8, 14), one likely explanation for the increased production of cytokines by *Mta2* null T cells is increased transcription of these genes caused by inactivation of the co-repressor complex. To explore this possibility, we analyzed the effects of *Mta2* inactivation on the expression of *IL-4* under stimulation by real-time PCR. Consistent with the increase in the protein levels (Figs. 4*E* and 6*B*), inactivation of Mta2 also resulted in an increase in the *IL-4* mRNA level (Fig. 6*C*). To determine whether the *IL-4* gene is a direct target of Mta2/NuRD, ChIP assays were performed using a polyclonal antibody against Mta2 in activated T cells. As a control for antibody specificity, rabbit IgG was also included in a parallel experiment. Data shown in Fig. 6*D* demonstrate that Mta2 binds to the promoter and downstream of the transcription start site (*lanes 2* and *5*). The ChIP signal is specific because a parallel ChIP assay using *Mta2* null cells did not enrich binding of Mta2. Based on these results, we conclude that the *IL-4* gene is a direct target of the Mta2-NuRD complex. The elevated expression of IFN-γ under Th2 conditions suggests that Mta2/NuRD likely suppress *IFN-γ* gene expression. However, we failed to detect direct binding of Mta2 to the *IFN-γ* promoter region (data not shown).

DISCUSSION

NuRD is a multisubunit protein complex that includes: Mta2, Mbd3, and Mi-2β, HDAC1/2 and RbAp46/48 (4, 9). NuRD is unique because it possesses both histone deacetylase and chromatin remodeling activities. To understand the *in vivo* function of this interesting complex, mice deficient in Mbd3 and Mi-2β, respectively, have been generated and characterized. Loss of Mbd3 function results in embryonic lethality and loss of ES cell pluripotency, suggesting a key function of NuRD in maintaining ES cell pluripotency and early embryogenesis (15, 16, 35). The phenotypes of T cell-specific Mi-2β knock-out revealed a critical role for Mi-2β in regulating *CD4* gene expression. However, instead of being a component of the NuRD co-repressor complex, Mi-2β appeared to activate *CD4* expression in T cells by association with p300 and HeLa E-box-binding protein (HEB) at the *CD4* enhancer (36). Therefore, the Mta2 knock-out mouse model presented here is the first model for understanding the function of the NuRD complex beyond embryonic development.

Based on production of autoantibodies, glomerulonephritis, skin lesions, and liver symptoms (Figs. 2 and 3), we conclude that *Mta2* null mice develop lupus-like autoimmune disease. Systemic lupus erythematosus is a major autoantibody-mediated autoimmune disease. Until now, the etiology of SLE remains unclear. Many knock-out and transgenic mouse models have provided important insights into the cellular and molecular mechanisms underlying lupus, and can be used to test potential lupus drugs. Genes that play important roles in SLE can be largely classified into several functional groups including: 1) apoptosis related, *e.g. Fas, Fas-L*, and *Bcl-2*; 2) T cell activation related, *e.g. CTLA4, PD1*, and *gadd45*; 3) B cell activation related, *e.g. Blys, Fyn*, and *Btk;* and 4) phagocytosis and debris clearance related, *e.g. c-Mer* and *DNase I*, and transcription factors such as *Aiolos*. The *Mta2* knock-out model described here is the first model to show that defects in chromatin remodeling and histone modification also cause lupus-like disease.

Inactivation of *Mta2*, although not affecting T cell development, causes T cell hyperproliferation upon TCR-mediated stimulation. Because the percentages of the naïve T cells, regu-

latory T cells, and memory T cells in peripheral are not affected by *Mta2* inactivation (Fig. 5*A* and data not shown), it is likely that Mta2 may be involved in controlling the threshold of T cell proliferation upon stimulation. This T cell phenotype has been observed in purified native CD4 T cells, in T cell-specific *Mta2* null mice, and in T cells from BMT SCID mice, suggesting a cell autonomous hyperproliferation. Consistent with this possibility, *Mta2* null mice exhibited autoimmune phenotypes. It is worth noting that *Mta2* null-BMT mice and TKO mice only recapitulate some of the *Mta2* null mice phenotypes, indicating that non-hematopoietic cells or non-T cells also contribute to the observed autoimmune disease in *Mta2* null mice. In a different study, we have found that *Mta2* null B cells exhibit severe developmental and differentiation defects (data not shown). However, those defects seem not to contribute to the autoimmune phenotypes observed in Mta2 null mice as B cell-specific knock-out mice do not exhibit any of the autoimmune phenotypes observed in *Mta2* conventional null mice.

In this study, we provide evidence supporting a role for Mta2 in modulating cytokine gene expression during T cell activation. It inhibits *IL-4* expression in Th2 cells, as a potential mechanism to prevent overproduction of IL-4 and Th2-related autoimmunity. In addition, we also demonstrate that *IL-4* is a direct target of Mta2 in T cells. Because Mta2 facilitates deacetylase activity of the NuRD complex (37), our observation that the *IL-4* expression level is increased in *Mta2* null T cells is consistent with the role of NuRD as a co-repressor. Future studies will address: (*a*) whether histone acetylation level at *IL-4* promoter is affected; (*b*) whether other components of NuRD are localized at this locus; and (*c*) whether *Mta2* deficiency affects chromatin remodeling activity of NuRD. Our data suggest that an *Mta2*-independent mechanism must be responsible for silencing the *IL-4* gene in Th1 cells. Our studies also indicate that Mta2/NuRD has a role in suppressing *IFN-γ* expression in Th2 cells. In Th2 cells, elevated IFN-γ is expressed in the presence of higher levels of IL-4, although direct binding of Mta2 to the *IFN-γ* gene is not detected. Thus, Mta2 may participate in suppressing *IFN-γ* gene expression via indirect mechanisms. Further characterization of other immune cell types in the *Mta2* null mice, identification of more Mta2/NuRD target genes, and epigenetic change occurred at the regulatory regions of these genes will give us a better picture of the role of Mta2/NuRD in the mammalian immune system.

Acknowledgments—We thank Dr. Hyung Kim and Dr. Virginia Godfrey for veterinary help and Manda Edwards for technical assistance.

REFERENCES

1. Margueron, R., Trojer, P., and Reinberg, D. (2005) *Curr. Opin. Genet. Dev.* **15,** 163–176
2. Martin, C., and Zhang, Y. (2005) *Nat. Rev. Mol. Cell. Biol.* **6,** 838–849
3. Cairns, B. R. (2005) *Curr. Opin. Genet. Dev.* **15,** 185–190
4. Feng, Q., and Zhang, Y. (2003) *Curr. Top. Microbiol. Immunol.* **274,** 269–290
5. Xue, Y., Wong, J., Moreno, G. T., Young, M. K., Cote, J., and Wang, W. (1998) *Mol. Cell* **2,** 851–861
6. Zhang, Y., LeRoy, G., Seelig, H. P., Lane, W. S., and Reinberg, D. (1998) *Cell* **95,** 279–289
7. Zhang, Y., Iratni, R., Erdjument-Bromage, H., Tempst, P., and Reinberg, D. (1997) *Cell* **89,** 357–364
8. Avitahl, N., Winandy, S., Friedrich, C., Jones, B., Ge, Y., and Georgopoulos, K. (1999) *Immunity* **10,** 333–343
9. Bowen, N. J., Fujita, N., Kajita, M., and Wade, P. A. (2004) *Biochim. Biophys. Acta* **1677,** 52–57
10. Wang, H., Cao, R., Xia, L., Erdjument-Bromage, H., Borchers, C., Tempst, P., and Zhang, Y. (2001) *Mol. Cell* **8,** 1207–1217
11. Kehle, J., Beuchle, D., Treuheit, S., Christen, B., Kennison, J. A., Bienz, M., and Muller, J. (1998) *Science* **282,** 1897–1900
12. Unhavaithaya, Y., Shin, T. H., Miliaras, N., Lee, J., Oyama, T., and Mello, C. C. (2002) *Cell* **111,** 991–1002
13. Hollander, M. C., Sheikh, M. S., Bulavin, D. V., Lundgren, K., Augeri-Henmueller, L., Shehee, R., Molinaro, T. A., Kim, K. E., Tolosa, E., Ashwell, J. D., Rosenberg, M. P., Zhan, Q., Fernandez-Salguero, P. M., Morgan, W. F., Deng, C. X., and Fornace, A. J., Jr. (1999) *Nat. Genet.* **23,** 176–184
14. Feng, Q., and Zhang, Y. (2001) *Genes Dev.* **15,** 827–832
15. Kaji, K., Caballero, I. M., Macleod, R., Nichols, J., Wilson, V. A., and Hendrich, B. (2006) *Nat. Cell. Biol.* **8,** 285–292
16. Kaji, K., Nichols, J., and Hendrich, B. (2007) *Development* **134,** 1123–1132
17. Solari, F., and Ahringer, J. (2000) *Curr. Biol.* **10,** 223–226
18. Fujita, N., Jaye, D. L., Kajita, M., Geigerman, C., Moreno, C. S., and Wade, P. A. (2003) *Cell* **113,** 207–219
19. Toh, Y., Oki, E., Oda, S., Tokunaga, E., Ohno, S., Maehara, Y., Nicolson, G. L., and Sugimachi, K. (1997) *Int. J. Cancer* **74,** 459–463
20. Toh, Y., Kuwano, H., Mori, M., Nicolson, G. L., and Sugimachi, K. (1999) *Br. J. Cancer* **79,** 1723–1726
21. Smale, S. T., and Fisher, A. G. (2002) *Annu. Rev. Immunol.* **20,** 427–462
22. Ansel, K. M., Lee, D. U., and Rao, A. (2003) *Nat. Immunol.* **4,** 616–623
23. Lee, G. R., Kim, S. T., Spilianakis, C. G., Fields, P. E., and Flavell, R. A. (2006) *Immunity* **24,** 369–379
24. Avni, O., Lee, D., Macian, F., Szabo, S. J., Glimcher, L. H., and Rao, A. (2002) *Nat. Immunol.* **3,** 643–651
25. Messi, M., Giacchetto, I., Nagata, K., Lanzavecchia, A., Natoli, G., and Sallusto, F. (2003) *Nat. Immunol.* **4,** 78–86
26. Fields, P. E., Lee, G. R., Kim, S. T., Bartsevich, V. V., and Flavell, R. A. (2004) *Immunity* **21,** 865–876
27. Hutchins, A. S., Mullen, A. C., Lee, H. W., Sykes, K. J., High, F. A., Hendrich, B. D., Bird, A. P., and Reiner, S. L. (2002) *Mol. Cell* **10,** 81–91
28. Lakso, M., Pichel, J. G., Gorman, J. R., Sauer, B., Okamoto, Y., Lee, E., Alt, F. W., and Westphal, H. (1996) *Proc. Natl. Acad. Sci. U. S. A.* **93,** 5860–5865
29. Kovalev, G. I., Franklin, D. S., Coffield, V. M., Xiong, Y., and Su, L. (2001) *J. Immunol.* **167,** 3285–3292
30. Kanauchi, H., Furukawa, F., and Imamura, S. (1991) *J. Investig. Dermatol.* **96,** 478–483
31. Lomvardas, S., and Thanos, D. (2002) *Cell* **110,** 261–271
32. Whitacre, C. C. (2001) *Nat. Immunol.* **2,** 777–780
33. Roubinian, J. R., Talal, N., Greenspan, J. S., Goodman, J. R., and Siiteri, P. K. (1978) *J. Exp. Med.* **147,** 1568–1583
34. Salvador, J. M., Hollander, M. C., Nguyen, A. T., Kopp, J. B., Barisoni, L., Moore, J. K., Ashwell, J. D., and Fornace, A. J., Jr. (2002) *Immunity* **16,** 499–508
35. Hendrich, B., Guy, J., Ramsahoye, B., Wilson, V. A., and Bird, A. (2001) *Genes Dev.* **15,** 710–723
36. Williams, C. J., Naito, T., Arco, P. G., Seavitt, J. R., Cashman, S. M., De Souza, B., Qi, X., Keables, P., Von Andrian, U. H., and Georgopoulos, K. (2004) *Immunity* **20,** 719–733
37. Zhang, Y., Ng, H. H., Erdjument-Bromage, H., Tempst, P., Bird, A., and Reinberg, D. (1999) *Genes Dev.* **13,** 1924–1935